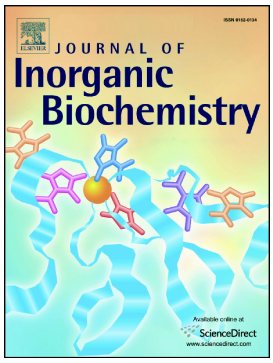

A metal-organic framework based PCR-free biosensor for the detection of gastric cancer associated microRNAs

Gui-Hua Qiu, Wan-Zhen Lu, Pei-Pei Hu, Zhi-Hong Jiang, Li-Ping Bai, Tao-Rui Wang, Min-Min Li, Jin-Xiang Chen

PII: S0162-0134(17)30486-5
DOI: doi: 10.1016/j.jinorgbio.2017.08.036
Reference: JIB 10322

To appear in: *Journal of Inorganic Biochemistry*

Received date: 5 July 2017
Revised date: 18 August 2017
Accepted date: 30 August 2017

Please cite this article as: Gui-Hua Qiu, Wan-Zhen Lu, Pei-Pei Hu, Zhi-Hong Jiang, Li-Ping Bai, Tao-Rui Wang, Min-Min Li, Jin-Xiang Chen , A metal-organic framework based PCR-free biosensor for the detection of gastric cancer associated microRNAs, *Journal of Inorganic Biochemistry* (2017), doi: 10.1016/j.jinorgbio.2017.08.036

A metal-organic framework based PCR-free biosensor for the detection of gastric cancer associated microRNAs

Gui-Hua Qiu [a, 1], Wan-Zhen Lu [a, 1], Pei-Pei Hu [a], Zhi-Hong Jiang [b], Li-Ping Bai [b], Tao-Rui Wang [c], Min-Min Li [c,*], Jin-Xiang Chen [a,*]

[a] *Guangdong Provincial Key Laboratory of New Drug Screening and Guangzhou Key Labotory of Drug Research for Emerging Virus Prevention and Treatment, School of Pharmaceutical Sciences, Southern Medical University, Guangzhou 510515, P. R. China*

E-mail: jxchen@smu.edu.cn

[b]*Macau Institute for Applied Research in Medicine and Health, Macau University of Science and Technology, Taipa, Macau*

[c]*Center of Clinical Laboratory, The First Affiliated Hospital of Jinan University, Guangzhou 510630, P. R. China*

Email: limm269@126.com

[1]*These authors contributed equally to this work*

Abstract We report herein five sensing platforms for the detection of five gastric cancer associated microRNAs (miRNAs). The sensing platforms are hybrids formed from a water-stable MOF $\{[Cu(dcbb)_2(H_2O)_2]\cdot 10H_2O\}_n$ (**1**, H_2dcbbBr = 1-(3,5-dicarboxybenzyl)-4,4'-bipyridinium bromide), respectively with five carboxyfluorescein (FAM) labeled probe single-stranded DNA (probe ss-DNA, denoted as P-DNA).Within the hybrid, MOF **1** tightly interacts with the P-DNA through electrostatic and/or π-stacking interactions and results in fluorescence quenching of FAM *via* a photo-induced electron transfer (PET) process. In the presence of the complementary target miRNAs *miR-185, miR-20a, miR-92b, miR-25*

and miR-210, which are expressed abnormally in the plasma of gastric carcinoma patients, P-DNA is released from the surface of MOF **1** ascribed to the stronger base pair matching, leading to the FAM fluorescence recovery. Each P-DNA@**1** system is effective and reliable for the detection of its complementary target miRNA with the detection limits from 91 to 559 pM, and is not interfered by other four miRNA sequences.

Keywords: Metal-organic framework; Fluorescence sensing; MiRNAs; Gastric cancer

1. Introduction

Gastric cancer (GC) is one of the most common malignancies and the third leading cause of cancer-related death globally [1]. The high mortality rate of GC is mainly due to the difficulty of early detection, and its diagnosis could only be done at the middle or late stage. At these stages, distant metastases and lymph node metastases are common [2]. Therefore, it is of urgent need to explore early diagnostic methods for GC to improve the survival rate of patients.

MicroRNA (miRNA) is considered as an important biomarker since abnormal expression of specific miRNA is associated with many diseases including cancer [3]. Therefore, it is important to develop biosensors to quantitatively detect miRNA expression levels in the early stage of disease. Recently, Min and coworkers have identified a five up-regulated miRNA signature (*miR-185*, *miR-20a*, *miR-92b*, *miR-25* and *miR-210*) in the plasma of GC patients that could serve as a non-invasive biomarker for the detection of GC [4]. Polymerase chain reaction (PCR), as an efficient DNA amplification *in vitro*, has been widely applied to detect miRNA. However, its assay processes are time-consuming, as this method includes a separate cDNA synthesis step prior to PCR, agarose gel analysis of PCR products, and in some instances, a second round of nested amplification or southern hybridization. The PCR amplification step increases the cost of the assay and the complexity of the detection. Moreover, post-PCR processing or nested PCR steps usually increase

the risk of false positive results due to carryover contamination [5]. As a consequence, it is extremely important to develop rapid and sensitive PCR-free sensing platforms with easily obtained materials to detect miRNA.

Metal-organic frameworks (MOFs) have aroused wide concern in the past decade [6-8]. The structures of these crystalline materials are composed of metal ions joined by a variety of multidentate organic ligands of broad levels of flexibility through strong covalent bonds. Correspondingly, MOFs have a wide range of applications in many fields, such as gas storage and separation [9-11], heterogeneous catalysis [12-14], sensing cations, anions and small molecules [15-18], drug delivery [19]. Employing MOFs as quenching platforms for the detection of disease-associated nucleic acids have been reported only very recently [20-25]. We have also found that MOFs based on zwitterionic quaternized-carboxylate ligands with two-dimensional (2D) or three-dimensional (3D) structures can be used as selective sensing platforms for the detection of ebolavirus RNA or HIV ds-DNA sequences *in vitro* [26-29]. This unique class of MOFs with cationic metal centers and conjugated polycarboxylate ligands can form π-stacking and/or electrostatic interactions with negatively charged probe DNA (P-DNA) sequences, thus result in a sensing platform for the detection of target disease-related RNA/DNA sequences [26-32]. Such sensing platform for nucleic acid detection offers advantage of high loading capacity of MOF for the P-DNA and resistance against P-DNA degradation [33].

In order to further investigate the structure of MOFs on the sensing efficiency, herein we reported a one dimensional (1D) double-stranded MOF $\{[Cu(dcbb)_2(H_2O)_2]\cdot 10H_2O\}_n$ (**1**, H_2dcbbBr = 1-(3,5-dicarboxybenzyl)-4,4'-bipyridinium bromide) bearing aromatic rings, positively charged pyridinium and uncoordinated carboxylates on its surface (Scheme 1), which can effectively associate with five respective P-DNA to give P-DNA@**1** hybrids. These hybrids can subsequently be used to distinguish their respective complementary miRNA which is expressed abnormally in the plasma of gastric carcinoma patients at picomolar level.

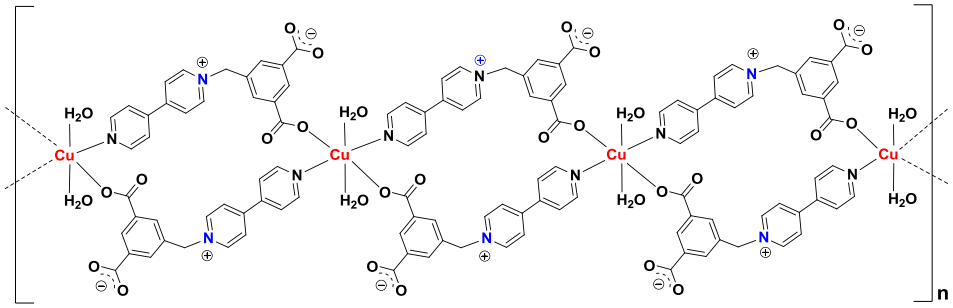

Scheme 1. The one-dimensional double-stranded structure of $\{[Cu(dcbb)_2(H_2O)_2]\cdot 10H_2O\}_n$ (**1**)

2 Experiment

2.1 General

MOF **1** was synthesized according to our reported procedures [26]. All the other reagents and solvents were obtained from commercial sources and used without further purification. All the DNA and RNA sequences were purchased from Sangon Inc. (Shanghai, China). The sequences are shown below.

Probe DNA-1 (P-DNA-1): 5'-TCAGGAACTGCCTTTCTCTCCA-FAM-3'

Complementary target RNA for P-DNA-1 (miR-185, T_1): 5'-UGGAGAGAAAGGCAGUUCCUGA-3'

Probe DNA-2 (P-DNA-2): 5'-CTACCTGCACTATAAGCACTTTA-FAM-3'

Complementary target RNA for P-DNA-2 (miR-20a, T_2): 5'-UAAAGUGCUUAUAGUGCAGGUAG-3'

Probe DNA-3 (P-DNA-3): 5'-GGAGGCCGGGACGAGTGCAATA-FAM-3'

Complementary target RNA for P-DNA-3 (miR-92b, T_3): 5'-UAUUGCACUCGUCCCGGCCUCC-3'

Probe DNA-4 (P-DNA-4): 5'-TCAGACCGAGACAAGTGCAATG-FAM-3'

Complementary target RNA for P-DNA-4 (miR-25, T_4): 5'-CAUUGCACUUGUCUCGGUCUGA-3'

Probe DNA-5 (P-DNA-5): 5'-TCAGCCGCTGTCACACGCACAG-FAM-3'

Complementary target RNA for P-DNA-5 (miR-210, T_5): 5'-CUGUGCGUGUGACAGCGGCUGA-3'

All the DNA and RNA samples were prepared in 100 μM Tris-HCl buffer solution (pH 7.4, 100 mM

NaCl, 5 mM $MgCl_2$) and stored at 4 °C for DNA or -80 °C for RNA.

2.2 Detection of miRNA

The fluorescence miRNAs sensing was performed at room temperature in 100 μM Tris-HCl (pH 7.4, 100 mM NaCl, 5 mM $MgCl_2$). Both of the excitation and emission slit widths are 10.0 nm. The fluorescence intensity at 518 nm with excitation at 480 nm was used for quantitative analysis. All the instruments were sterilized in the autoclavable container. The fluorescence quenching efficiency (Q_E) and recovery efficiency (R_E) were tested and calculated according to our reported procedures [26-29].

The binding constant of each P-DNA or P-DNA/RNA hybrid duplex with MOF **1** is calculated *via* the following double logarithm Eq. (1),

$$\log\frac{F_0 - F}{F} = n\log[\mathbf{1}] + \log K_b \quad (1)$$

wherein F_0 and F are the fluorescence intensities at 518 nm in the absence and presence of MOF **1**, K_b is the binding constant and n is the number of binding sites.

Each experiment was carried out three times, and the mean values were taken.

3 Results and discussion

In terms of the structure of MOF **1**, it shows a 1D structure with cationic Cu(II) center, the conjugated dicarboxylate ligand of dcbb (dcbb = 1-(3,5-dicarboxybenzyl)-4,4'-bipyridinium) bearing positively charged pyridinium and uncoordinated carboxylates and the 1D structure of **1** allows a maximum exposure of these functionalities to P-DNAs. These features are advantageous in forming π-stacking, electrostatic interactions and/or hydrogen bonding with negatively charged P-DNA sequences. The P-DNA@**1** hybrid systems can therefore effectively formed for the detection of the complementary target disease-related RNA/DNA sequences [20-25]. To test this hypothesis, we select five types of FAM-labeled ss-DNAs as P-DNAs (FAM = carboxyfluorescein), which are the complementary sequences for miRNAs (*miR-185*, *miR-20a*, *miR-92b*,

miR-25 and *miR-210*) that are expressed abnormally in the plasma of gastric carcinoma patients [4]. As shown in Fig. 1, the fluorescence intensity of the each P-DNA decreases upon addition of MOF **1** with the quenching efficiency (Q_E) being (87±5)% for P-DNA-1, (94±3)% for P-DNA-2, (77±8)% for P-DNA-3, (95±2)% for P-DNA-4 and (96±4)% for P-DNA-5 with saturation concentrations of MOF **1** being 52 μM, 85 μM, 65 μM, 60 μM, and 35 μM, respectively. As listed in Table 1, the slightly lower quenching efficiency for P-DNA-3 is likely due to its lower binding ability and less binding sites ($K_b = 5.8\times10^3\ M^{-1}$, n = 0.98) than those of P-DNA-1 ($K_b = 8.8\times10^3\ M^{-1}$, n = 1.6), P-DNA-2 ($K_b = 1.2\times10^4\ M^{-1}$, n = 1.5), P-DNA-4 ($K_b = 3.5\times10^4\ M^{-1}$, n = 1.5) and P-DNA-5 ($K_b = 5.3\times10^4\ M^{-1}$, n = 1.3) toward MOF **1**. MOF **1** quenches the fluorescence of P-DNAs fluorescence through π-stacking, electrostatic interactions and/or hydrogen bonding indicating a static quenching procedure [30-32], therefore, their binding constants are calculated *via* the double logarithm Eq. (3) [34-35].

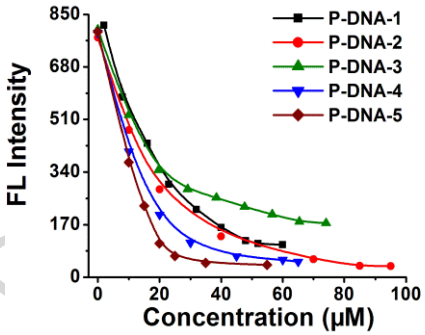

Fig. 1 Fluorescence intensity quenching of the P-DNAs incubated with MOF **1** of varying concentrations in 100 μM Tris-HCl buffer solution (pH 7.4, 100 mM NaCl, 5 mM $MgCl_2$) at room temperature (λ_{ex} = 480, λ_{em} = 518).

In principle, introduction of the relevant complementary target miRNA to the corresponding P-DNA@**1** system would lead to the formation of stable and rigid P-DNA@RNA hybrid duplex. The formation of P-DNA@RNA hybrid duplex compels the P-DNA away from the surface of **1**, thereby blocking the PET process and leading to the fluorescence recovery [30-32]. Following this assumption, we evaluated P-DNAs@**1** systems as sensing platforms for the target miRNAs by the fluorescence recovery upon addition

of complementary target miRNA T_1 to T_5. As shown in Fig. S1, with the lowest concentration of 25 nM, the fluorescence intensity increased with incubation time and exhibited no further increase after 13±3 min for T_1, 14±2 min for T_2, 15±2 min for T_3, 19±1 min for T_4 and 38±3 min for T_5, showing that the system reached equilibrium between P-DNA@**1** and the P-DNA@target miRNA. Thus, 13 min, 14 min, 15 min, 19 min and 38 min were chosen as the incubation time for the detection of five types of target miRNAs, respectively. The longer fluorescence recovery time for P-DNA-5@**1** is likely due to the stronger binding ability between **1** and P-DNA-5 ($K_b = 5.3\times10^4$ M^{-1}, Table 1). As shown in Fig. 2, with more target miRNAs added, more P-DNAs are released and caused a gradual increase in the fluorescence intensity. In addition, saturation in the fluorescence recovery was observed at the concentration of 80 nM for T_1 and T_5, 100 nM for T_2 and T_3, 70 nM for T_4 as shown in Fig. S2. Under this condition, the fluorescence intensity shows good linear relationship with the concentration of the target miRNAs (Insets of Fig. S2), giving the detection limits of 172±5 pM for T_1, 321±8 pM for T_2, 91±7 pM for T_3, 559±8 pM for T_4, and 132±12 pM for T_5.

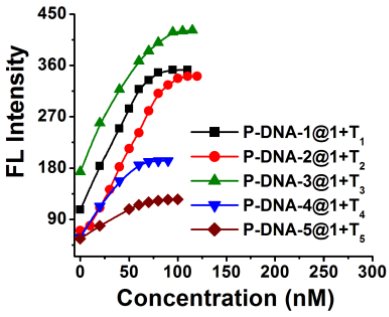

Fig. 2 The fluorescence intensity of P-DNAs@**1** at 518 nm *versus* the concentrations of T_1 to T_5.

The specificity and cross-reactivity of P-DNA@**1** systems are further studied. Five P-DNA@**1** sensing systems were prepared accordingly. Then a solution contains complementary target miRNA only, or complementary target miRNA mixed with the other four non-complementary miRNA, or four non-complementary miRNAs, was added respectively to each of the above prepared sensing system. The results are shown in Fig.3, as expected, solution containing complementary target miRNA only, or a

admixture of complementary target miRNA and four non-complementary miRNAs results in significant fluorescence enhancement with the recovery efficiency (R_E) reaching 2.4±0.12 and 2.0±0.09 for P-DNA-1@**1**, 3.3±0.15 and 2.8±0.13 for P-DNA-2@**1**, 1.5±0.12 and 0.8±0.11 for P-DNA-3@**1**, 1.8±0.13 and 1.0±0.09 for P-DNA-4@**1**, 1.2±0.08 and 0.8±0.05 for P-DNA-5@**1**. Under similar conditions for a solution containing four non-complementary miRNAs, the R_E values are only 0.08 for P-DNA-1@**1** and P-DNA-2@**1**, 0.06 for P-DNA-3@**1** and P-DNA-4@**1**, 0.02 for P-DNA-5@**1**, respectively. These results convincingly suggest that each P-DNA@**1** system functions as a highly selective sensing platform for the detection of complementary target miRNA with negligible cross-reactivity with non-complementary miRNAs.

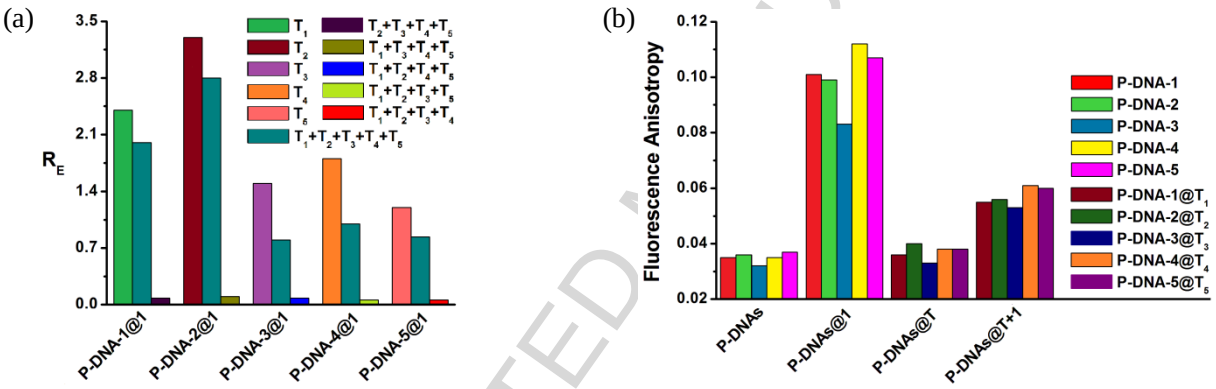

Fig. 3 (a) The sequence specificity and cross-reactivity of the proposed miRNA sensor of P-DNAs@**1**. (b) Fluorescence anisotropy of P-DNA (50 nM), P-DNA@T (50 nM/50 nM) before and after the addition of MOF **1** (52 μM for P-DNA-1 and P-DNA-1@T_1, 85 μM for P-DNA-2 and P-DNA-2@T_2, 65 μM for P-DNA-3 and P-DNA-3@T_3, 60 μM for P-DNA-4 and P-DNA-4@T_4, 35 μM for P-DNA-5 and P-DNA-5@T_5) with an incubation time of 13, 14, 15, 19 and 38 min, respectively.

The above results may be rationalized from the unique structure of **1** with zeta potential of +4.2 mV meaning being positively charged [36-39]. Thus, **1** can absorb P-DNAs through electrostatic, π-stacking and/or hydrogen-bonding interactions to form P-DNAs@**1** complexes [40-42], and thus quench the fluorescence of the FAM moiety *via* a PET process [43-47]. Upon addition of the complementary target miRNA and subsequent DNA@RNA duplex formation, MOF **1** lost the capacity of association due to the

more rigid nature of the duplex as well as the significant loss of unpaired nucleobases [41]. Therefore, the competitive hybridization of complementary RNA with the absorbed P-DNA would lead to the release of the FAM-labeled P-DNA from **1**, resulting in the restoration of fluorescence (Scheme 2).

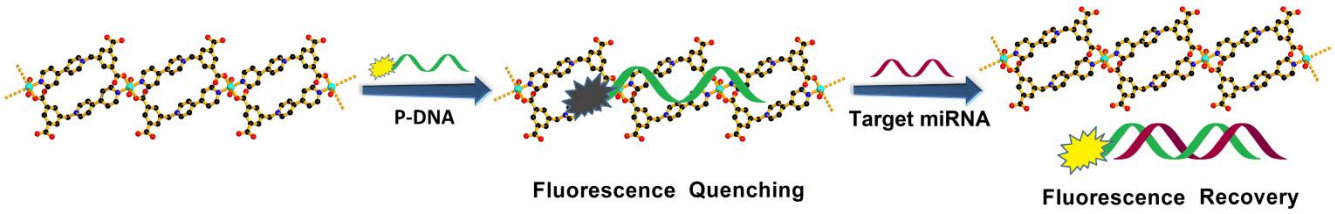

Scheme 1. Proposed mechanism for the detection of target miRNA sequences based on a fluorescent biosensor formed from MOF **1** and fluorophore-labeled probe DNA.

The proposed mechanism was firstly supported by the changes of the fluorescence anisotropy (FA) of the P-DNAs, and P-DNA@RNA duplex before and after the addition of MOF **1**. It is known that fluorescence anisotropy can be a measure of the rotational motion-related factors of fluorophore-labeled DNA [48-50], and is herein invoked as a means to judge whether a P-DNA is attached to the surface of MOF **1**. As shown in Fig. 3b, addition of **1** into the solution of P-DNAs leads to an increase in FA by factors of 0.10 for both P-DNA-1 and P-DNA-2, 0.08 for P-DNA-3, 0.11 for both P-DNA-4 and P-DNA-5, whereas 0.06 for P-DNA-1@T_1, P-DNA-2@T_2, 0.05 for P-DNA-3@T_3, P-DNA-4@T_4 and P-DNA-5@T_5. These results reveal a stronger interaction of **1** with the P-DNAs than with hybrid DNA@RNA duplexes.

Secondly, the stronger interactions of P-DNAs with **1** than those of DNA@RNA duplexes with **1** also corroborated by the binding constants listed in Table 1. With approximately similar binding sites for each couple of P-DNA and P-DNA@T with MOF **1**, the binding ability for MOF **1** with P-DNA-1 is 3.5 times of P-DNA-1@T_1, P-DNA-2 is 2.0 times of P-DNA-2@T_2, P-DNA-3 is 3.4 times of P-DNA-3@T_3, P-DNA-4 is 8.9 times of P-DNA-4@T_4, P-DNA-5 is 8.0 times of P-DNA-5@T_5.

Table 1 Binding parameters of P-DNAs and DNA@RNA hybrid duplexes with MOF **1**.

	K_b($\times 10^4$ M^{-1})	n	R^2
P-DNA-1	0.88	1.6	0.9991
P-DNA-1@T_1	0.25	1.6	0.9960
P-DNA-2	1.19	1.5	0.9986
P-DNA-2@T_2	0.57	1.3	0.9839
P-DNA-3	0.58	0.95	0.9865
P-DNA-3@T_3	0.17	0.82	0.9959
P-DNA-4	3.5	1.5	0.9934
P-DNA-4@T_4	0.39	1.4	0.9959
P-DNA-5	5.3	1.3	0.9939
P-DNA-5@T_5	0.67	1.2	0.9789

Thirdly, agarose gel electrophoresis was carried out to further confirm that P-DNA exhibit stronger affinity toward **1** than hybrid DNA@RNA duplex. As shown in Fig. 4,. P-DNA-1 or T_1 displays one light band with strong fluorescence. By contrast, no light band was observed when P-DNA-1 was incubated with MOF **1**, suggesting that P-DNA-1 can integrate with MOF **1** and the formed P-DNA-1@**1** ensemble was too large to pass through the gel [51-52]. Once T_1 was introduced, the hybridization products of P-DNA-1 exhibited two light bands. The brighter one represents the hybrid duplex DNA@RNA which possesses higher molecular weight and moved slower, while the darker one represents the remaining excessive un-hybridized T_1 which possesses lower molecular weight and moved faster. However, two light bands were visible if MOF **1** was employed after the hybridization of P-DNA-1 with T_1, which attributed to that the hybrid duplex DNA@RNA has weaker affinity toward MOF **1** and then penetrate into the gel with excessive T_1 band [53]. Similar observations were made for other four couples of P-DNA and P-DNA@T. These experiments further certificated that MOF **1** can distinguish P-DNA from hybrid duplex DNA@RNA and effectively verified the proposed mechanism.

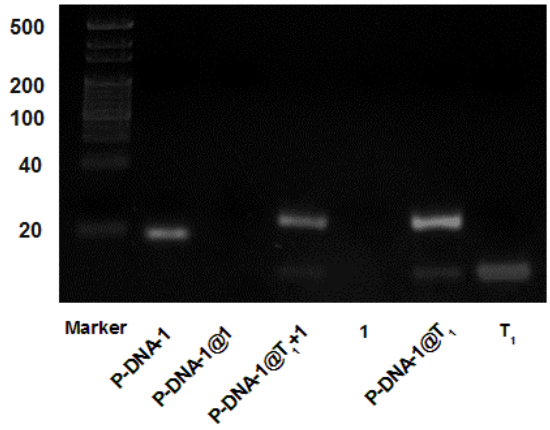

Fig. 4 Gel electrophoresis of P-DNA-1 (50 nM), P-DNA-1@T_1 (50 nM/80 nM), before and after the addition of MOF **1** (52 μM) and T_1 (80 nM) as control.

4 Conclusions

In summary, we present in this paper a miRNA sensing array composed of fluorophore-labeled P-DNAs that are hybridized with a 1D MOF as a fluorescence quencher. In the presence of target miRNA, P-DNA is hybridized with target miRNA and released from the MOF, leading to the recovery of fluorescence. The formed five P-DNA@**1** sensing systems not only enable the quantitative and highly specific detection of complementary target miRNAs, but also not interfered by the other miRNAs. Our advantage comes from the use of inexpensive MOF, the alleviation of laborious preparation, as well as the facile direct detection procedures which is critical for further in situ analysis of living cells. We anticipate that this study will advance the understanding of miRNA functionality in a vast range of biological processes and benefit early disease diagnostics and drug discovery to improve human health.

Acknowledgements

We are grateful for the financial support from the Guangdong Provincial Department of Science and Technology of China (2015A010105016) and Guangdong Provincial Natural Science Foundation of China (2015A030313284), the open project of State Key Laboratory of Quality Research in Chinese Medicine

(Macau University of Science and Technology, MUST-SKL-2016-04) funded by the Macao Science and Technology Development Fund, Macau Special Administrative Region, and Special Funds for the Cultivation of Guangdong College Students' Scientific and Technological Innovation. ("Climbing Program" Special Funds).

References

[1] J. Ferlay, I. Soerjomataram, R. Dikshit, S. Eser, C. Mathers, M. Rebelo, D.M. Parkin, D. Forman, F. Bray, Int. J. Cancer 136 (2015) 359−386.

[2] C. Jackson, D. Cunningham, J. Oliveira, Ann. Oncol. 20 (2009) 34−36.

[3] S.B. Lin, R.I. Gregory, Nat. Rev. Cancer 15 (2015) 321−333.

[4] X. Zhou, W. Zhu, H. Li, W. Wen, W.F. Cheng, F. Wang, Y.X. Wu, L.W. Qi, Y. Fan, Y. Chen, Y. Ding, J. Xu, J.Q. Qian, Z.B. Huang, T.S. Wang, D.X. Zhu, Y.Q. Shu, P. Liu, Sci. Rep. 5 (2015) 11251−11264.

[5] H. Kobayashi, M. Oethingera, M.J. Tuohy, G.W. Procopa, G.S. Halla, T.W. Bauer, Diagn. Microbiol. Infec. Dis. 64 (2009) 445−447.

[6] C.B. He, D.M. Liu, W.L. Lin, Chem. Rev. 115 (2015) 11079−11108.

[7] J.R. Li, J. Sculley, H.C. Zhou, Chem. Rev. 112 (2012) 869−932.

[8] W.H. Zhang, Z.G. Ren, J.P. Lang,.Chem. Soc. Rev. 45(2016) 4995−5019.

[9]T. Rodenas, I. Luz, G. Prieto, B. Seoane, H. Miro, A. Corma, F. Kapteijn, F.X. Llabrés i Xamena, J. Gascon, Nat. Mater. 14 (2015) 48−55.

[10] D. Liu, J.P. Lang, B.F. Abrahams, J. Am. Chem. Soc. 133 (2011) 11042−11045.

[11] J.P. Lang, Q.F. Xu, R.X. Yuan, B.F. Abrahams, Angew. Chem., Int. Ed., 43 (2004) 4741−4745.

[12] H.X. Li, W. Zhang, H.Y. Li, Z.L. Xu, W.X. Wang, J.P. Lang, Chem. Commun. 49 (2013) 4259−4261.

[13] Y.Q. Yuan, F.L. Yuan, F.L. Li, Z.M. Hao, J. Guo, D.J. Young, W.H. Zhang, J.P. Lang, Dalton Trans. 46 (2017) 7154−7158.

[14] F.L. Li, H.X. Li, J.P. Lang, CrystEngComm, 18 (2016) 1760−1767.

[15] Y.X. Shi, W.X. Li, H.H. Chen, D.J. Young, W.H. Zhang, J.P. Lang, Chem. Commun. 53 (2017) 5515−5518.

[16] M. Dai, X.R. Su, X. Wang, B. Wu, Z.G. Ren, X. Zhou, J.P. Lang, Inorg. Chem. 56 (2017) 4668−4678.

[17] F. Wang, Y.T. Wang, H. Yu, J.X. Chen, B.B. Gao, J.P. Lang, Inorg. Chem. 55 (2016) 9417−9423.

[18] M.M Chen, L. Chen, H.X. Li, L. Brammer, J.P. Lang, Inorg. Chem. Frontiers 3 (2016) 1297−1305.

[19] T. Kundu, S. Mitra, P. Patra, A. Goswami, D. DÍaz DÍaz, R. Banerjee, Mechanical downsizing of a gadolinium (III)-based metal-organic framework for anticancer drug delivery, Chem. Eur. J. 20 (2014) 10514−10518.

[20] X. Zhu, H.Y. Zheng, X.F. Wei, Z.Y. Lin, L.H. Guo, B. Qiu, G.N. Chen, Metal-organic framework (MOF): a novel sensing platform for biomolecules, Chem. Commun. 49 (2013) 1276−1278.

[21] C.Q. Zhao, L. Wu, J.S. Ren, Y. Xu, X.G. Qu, Targeting human telomeric higher-order DNA: dimeric G-quadruplex units serve as preferred binding site, J. Am. Chem. Soc. 135 (2013) 18786−18789.

[22] H.T. Zhang, J.W. Zhang, G. Huang, Z.Y. Du, H.L. Jiang, An amine-functionalized metal-organic framework as a sensing platform for DNA detection, Chem. Commun. 50 (2014) 12069−12072.

[23] J.Q. Tian, Q. Liu, J.L. Shi, J.M. Hu, A.M. Asiri, X.P. Sun, Y.Q. He, Rapid, sensitive, and selective fluorescent DNA detection using iron-based metal-organic framework nanorods: Synergies of the metal center and organic linker, Biosens. Bioelectron. 71 (2015) 1−6.

[24] Y.F. Wu, J.Y. Han, P. Xue, R. Xu, Y.J. Kang, Nano metal-organic framework (NMOF)-based strategies for multiplexed microRNA detection in solution and living cancer cells, Nanoscale 7 (2015) 1753−1759.

[25] L. Chen, H. Zheng, X. Zhu, Z. Lin, L. Guo, B. Qiu, G. Chen, Z.N. Chen, Metal-organic frameworks-based biosensor for sequence-specific recognition of double-stranded DNA, Analyst 138 (2013) 3490−3493.

[26] H.Q. Zhao, S.P. Yang, N.N. Ding, L. Qin, G.H. Qiu, J.X. Chen, W.H. Zhang, W.H. Chen, T. S. Andy Hor, A zwitterionic 1D/2D polymer co-crystal and its polymorphic sub-components: a highly selective sensing platform for HIV ds-DNA sequences, Dalton Trans. 45 (2016) 5092−5100.

[27] L. Qin, L.X. Lin, Z.P. Fang, S.P. Yang, G.H. Qiu, J.X. Chen, W.H. Chen, A water-stable metal-organic framework of a zwitterionic carboxylate with dysprosium: a sensing platform for Ebolavirus RNA sequences, Chem. Commun. 52 (2016) 132−135.

[28] S.P. Yang, S.R. Chen, S.W. Liu, X.Y. Tang, L. Qin, G.H. Qiu, J.X. Chen, W.H. Chen, Platforms formed from a three-dimensional Cu-based zwitterionic Metal-organic framework and probe ss-DNA: selective fluorescent biosensors for human immunodeficiency virus 1 ds-DNA and Sudan virus RNA sequences, Anal. Chem. 87 (2015) 12206−12214.

[29] H.Q. Zhao, G.H. Qiu, Z. Liang, M.M. Li, B. Sun, L. Qin, S.P. Yang, W.H. Chen, J.X. Chen, A zinc(II)-based two-dimensional MOF for sensitive and selective sensing of HIV-1 ds-DNA sequences, Anal. Chim. Acta 922 (2016) 55−63.

[30] Y. Cui, Y. Yue, G. Qian, B. Chen, Luminescent functional metal-organic frameworks, Chem. Rev. 112 (2011) 1126−1162.

[31] G.Y. Wang, C. Song, D.M. Kong, W.J. Ruan, Z. Chang, Y. Li, Two luminescent metal-organic frameworks for the sensing of nitroaromatic explosives and DNA strands, J. Mater. Chem. A 2 (2014) 2213−2220.

[32] W. Morris, W.E. Briley, E. Auyeung, M.D. Cabezas, C.A. Mirkin, Nucleic acid-metal organic framework (MOF) nanoparticle conjugates, J. Am. Chem. Soc. 136 (2014) 7261−7264.

[33] C. He, K. Lu, D. Liu, W. Lin, Nanoscale metal-organic frameworks for the co-delivery of cisplatin and pooled siRNAs to enhance therapeutic efficacy in drug-resistant ovarian cancer cells, J. Am. Chem. Soc. 136 (2014) 5181−5184.

[34] N. Akbay, Z. Seferoğlu, E. Gök, Fluorescence interaction and determination of calf thymus DNA with two ethidium derivatives, J. Fluoresc. 19 (2009) 1045−1051.

[35] S. Kashanian, J.E.N. Dolatabadi, In vitro studies on calf thymus DNA interaction and 2-tert-butyl-4-methylphenol food additive, Eur. Food Res. Technol. 230 (2010) 821−825.

[36] R. Deleurence, C. Parneix, C. Monteux, Mixtures of latex particles and the surfactant of opposite charge used as interface stabilizers-influence of particle contact angle, zeta potential, flocculation and shear energy, Soft Matter 10 (2014) 7088−7095.

[37] H. Lakhotiya, K. Mondal, R.K. Nagarale, A. Sharma, Low voltage non-gassing electro-osmotic pump with zeta potential tuned aluminosilicate frits and organic dye electrodes, RSC Adv. 4 (2014) 28814−28821.

[38] M. Ferriz-Mañas, J.B. Schlenoff, Zeta potential of polyelectrolyte multilayers using the spinning disk method, Langmuir 30 (2014) 8776−8783.

[39] A. Mikolajczyk, A. Gajewicz, B. Rasulev, N. Schaeublin, E. Maurer-Gardner, S. Hussain, J. Leszczynski, T. Puzyn, Zeta potential for metal oxide nanoparticles: a predictive model developed by a nano-quantitative structure-property relationship approach, Chem. Mater. 27 (2015) 2400−2407.

[40] Y. Cui, Y. Yue, G. Qian, B. Chen, Luminescent functional metal-organic frameworks, Chem. Rev. 112 (2011) 1126−1162.

[41] G.Y. Wang, C. Song, D.M. Kong, W.J. Ruan, Z. Chang, Y. Li, Two luminescent metal-organic frameworks for the sensing of nitroaromatic explosives and DNA strands, J. Mater. Chem. A 2 (2014) 2213−2220.

[42] W. Morris, W.E. Briley, E. Auyeung, M.D. Cabezas, C.A. Mirkin, Nucleic acid–metal organic framework (MOF) nanoparticle conjugates, J. Am. Chem. Soc. 136 (2014) 7261−7264.

[43] S.X. Jiang, H. Yan, Y. Liu, Kinetics of DNA tile dimerization, ACS Nano. 8 (2014) 5826−5832.

[44] C. Wang, Y.L. Tang, Y. Guo, Adenosine deaminase biosensor combining cationic conjugated polymer-based FRET with deoxyguanosine-based photoinduced electron transfer, ACS Appl. Mater. Interfaces 6 (2014) 21686−21691.

[45] E.K. Lim, T. Kim, S. Paik, S. Haam, Y.M. Huh, K. Lee, Nanomaterials for theranostics: recent advances and future challenges, Chem. Rev. 115 (2014) 327−394.

[46] J. Zheng, R. Yang, M. Shi, C. Wu, X. Fang, Y. Li, J. Li, W. Tan, Rationally designed molecular beacons for bioanalytical and biomedical applications, Chem. Soc. Rev. 44 (2015) 3036−3055.

[47] A.P. de Silva, H.Q. Gunaratne, T. Gunnlaugsson, A.J. Huxley, C.P. McCoy, J.T. Rademacher, T.E. Rice, Signaling recognition events with fluorescent sensors and switches, Chem. Rev. 97 (1997) 1515−1566.

[48] L.H. Tang, H.X. Chang, Y. Liu, J.H. Li, Duplex DNA/graphene oxide biointerface: from fundamental understanding to specific enzymatic effects, Adv. Funct. Mater. 22 (2012) 3083−3088.

[49] J.F. Guo, C.M. Li, X.L. Hu, C.Z. Huang, Y.F. Li, Metal-organic framework MIL-101 enhanced fluorescence anisotropy for sensitive detection of DNA, RSC Adv. 4 (2014) 9379−9382.

[50] J.M. Fang, F. Leng, X.J. Zhao, X.L. Hua, Y.F. Li, Metal-organic framework MIL-101 as a low background signal platform for label-free DNA detection, Analyst 139 (2014) 801−806.

[51] J.F. Guo, C.M. Li, X.L. Hu, C.Z. Huang, Y.F. Li, Metal-organic framework MIL-101 enhancedfluorescence anisotropy for sensitive detection of DNA, RSC Adv. 4 (2014) 9379−9382.

[52] J.H. Liu, C.Y. Wang, Y. Jiang, Y.P. Hu, J.S. Li, S. Yang, Y.H. Li, R.H. Yang, W.H. Tan, C.Z. Huang, Graphene signal amplification for sensitive and real-time fluorescence anisotropy detection of small molecules, Anal. Chem. 85 (2013) 1424−1430.

[53] P.J.J. Huang, J.W. Liu, Separation of short single-and double-stranded DNA based on their adsorption kinetics difference on graphene oxide, J. Nanomater. 3 (2013) 221−228.

Graphical Abstract

A metal-organic framework based PCR-free biosensor for the detection of gastric cancer associated microRNAs

Gui-Hua Qiu, Wan-Zhen Lu, Pei-Pei Hu, Zhi-Hong Jiang, Li-Ping Bai, Tao-Rui Wang, Min-Min Li*, Jin-Xiang, Chen*

Five sensing platforms were formed from MOF **1**, respectively with five carboxyfluorescein labeled ss-DNA. These sensing platforms can be used for the detection of five type miRNAs, which are expressed abnormally in the plasma of gastric carcinoma patients. Each sensing system is effective and reliable for the detection of its complementary target miRNA with the detection limits from 91 to 559 pM, and is not interfered by the other four miRNA sequences.

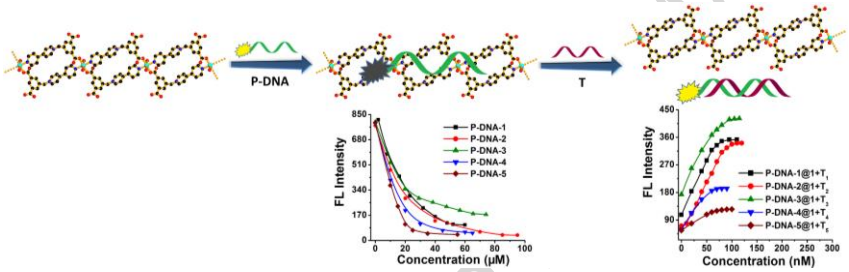

Highlights

A metal-organic framework based PCR-free biosensor for the detection of gastric cancer associated microRNAs

Gui-Hua Qiu, Wan-Zhen Lu, Pei-Pei Hu, Zhi-Hong Jiang, Li-Ping Bai, Tao-Rui Wang, Min-Min Li*, Jin-Xiang, Chen*

Research Highlights

►Five sensing platforms were formed from MOF **1**, respectively with five probe DNA.

►These sensing platforms can be used for the detection of five type miRNAs related to gastric carcinoma.

►Each sensing system is selectively for the detection of its complementary miRNA.

►The detection limits are from 91 to 559 pM.